Ablation Lesion Assessment with MRI

Lluís Mont [iD],[1,2,3] Ivo Roca-Luque [iD][1,2,3] and Till F Althoff [iD][1,2,4,5]

1. Arrhythmia Section, Cardiovascular Institute, Clínic – University Hospital Barcelona, Barcelona, Catalonia, Spain; 2. Institut d'Investigacions Biomèdiques August Pi i Sunyer (IDIBAPS), Barcelona, Catalonia, Spain; 3. Centro de Investigación Biomédica en Red Cardiovascular (CIBERCV), Madrid, Spain; 4. Department of Cardiology and Angiology, Charité University Medicine Berlin, Berlin, Germany; 5. German Centre for Cardiovascular Research (DZHK), Berlin, Germany

Abstract

Late gadolinium enhancement (LGE) MRI is capable of detecting not only native cardiac fibrosis, but also ablation-induced scarring. Thus, it offers the unique opportunity to assess ablation lesions non-invasively. In the atrium, LGE-MRI has been shown to accurately detect and localise gaps in ablation lines. With a negative predictive value close to 100% it can reliably rule out pulmonary vein reconnection non-invasively and thus may avoid unnecessary invasive repeat procedures where a pulmonary vein isolation only approach is pursued. Even LGE-MRI-guided repeat pulmonary vein isolation has been demonstrated to be feasible as a standalone approach. LGE-MRI-based lesion assessment may also be of value to evaluate the efficacy of ventricular ablation. In this respect, the elimination of LGE-MRI-detected arrhythmogenic substrate may serve as a potential endpoint, but validation in clinical studies is lacking. Despite holding great promise, the widespread use of LGE-MRI is still limited by the absence of standardised protocols for image acquisition and post-processing. In particular, reproducibility across different centres is impeded by inconsistent thresholds and internal references to define fibrosis. Thus, uniform methodological and analytical standards are warranted to foster a broader implementation in clinical practice.

Late gadolinium enhancement (LGE) cardiac MRI is increasingly used to detect cardiac fibrosis in the context of arrhythmias.[1–4] Fibrosis is a hallmark of arrhythmogenic cardiac remodelling and constitutes an important substrate in both atrial and ventricular arrhythmias.[2,3]

Of note, by exploiting the slow washout kinetics of gadolinium in extracellular space, LGE-MRI is not only capable of determining native fibrotic tissue, but also of detecting ablation-induced scarring.[5–13] Several groups have reported LGE-MRI-based localisation of functional gaps in atrial ablation lesions with high accuracy, and even LGE-MRI-guided repeat pulmonary vein isolation (PV) has been demonstrated to be efficient and effective as a standalone approach.[5,7,14] Although the use of LGE-MRI for ventricular ablation lesion assessment is lagging behind compared to the atrium, feasibility has been demonstrated in preclinical and early clinical studies.[10,15,16] However, initial data on the accuracy of LGE-MRI-based lesion assessment were somewhat conflicting.[5,6,17,18] This limited reproducibility of promising results across centres may have been because of differences in the methods of image acquisition, post-processing and analysis.[19] In addition, we have generated evidence that the timing of image acquisition with respect to different stages of lesion formation and scar remodelling also has to be considered.[20]

This review focuses on the assessment of chronic ablation lesions using LGE-MRI and its utility in clinical practice. The scope of this article does not include real-time monitoring of lesion formation through intraprocedural MRI, which – despite holding great promise – is still of limited clinical relevance because of current structural and technical limitations related to electromagnetic interference, as well as the relative absence of acute parameters that accurately predict definite lesion formation.[21]

Pathology of Lesion Formation

The pathology of radiofrequency (RF) ablation injury is well established in animal models and patients and is characterised by coagulation necrosis, haemorrhage and complete loss of cellular and vascular architecture, apart from a narrow peripheral transition zone.[9,22–25] The response to ablation injury implies infiltration of immune cells and neovascularisation, with local inflammation and interstitial oedema being observed up to 8 weeks post-ablation.[11,23,25] In parallel, activated fibroblasts proliferate and differentiate into myofibroblasts that generate fibrogenic signals, which perpetuate tissue repair and promote collagen deposition resulting in replacement of myocardium with fibrous scar tissue.[22,24–26] While RF ablation and cryoablation fundamentally differ in the acute effect on the tissue and the mechanism of cell death, most of these basic principles of

Table 1: Image Post-processing (Normalisation and Thresholds to Define Lesions)

	Internal Reference for Normalisation	Thresholds Defining Atrial Lesions	Image Acquisition
Atrial Lesion Assessment			
Oakes et al. 2009[39]	Normal tissue ("lower region of the pixel intensity histogram between 2% and 40% of the maximum intensity within the region of interest [e.g. the left atrial wall]")	User-selected individual threshold (2–4 SD above the mean of 'normal'†, based on the investigators' discretion)	1.5 T, 15 min post gadolinium (0.1 mmol/kg Multihance [Braco Diagnostic],* 0.5 M)
Khurram et al. 2014[50]	Mean LA blood pool signal intensity	Universal threshold (upper limit of normal: IIR 0.97; dense scar: >1.6)	1.5 T, 15–25 min post gadolinium (0.2 mmol/kg Magnevist [Bayer],* 0.5 M)
Benito et al. 2017[38]	Mean LA blood pool signal intensity	Universal threshold (upper limit of normal: IIR 1.2; dense scar: >1.32)	3 T, 20 min post gadolinium (0.2 mmol/kg Gadovist [Bayer], 1.0 M)
Harrison et al. 2015[17]	Mean LA blood pool signal intensity	No fixed threshold, but visualisation of signal intensities in SD from reference	1.5 T, 20 min post gadolinium (0.2 mmol/kg Gadovist, 1.0 M)
Jefairi et al. 2019[51]	Maximum signal intensity	Universal threshold with possible individual adaptation (>50% maximum signal intensity)	1.5 T, 17 min post gadolinium (0.2 mmol/kg Dotarem [Guerbet], 0.5 M)
Peters et al. 2007[40]	LA blood pool signal intensity	"Minimum threshold which eliminates most left atrial blood pool pixels"	1.5 T, 20–25 min post gadolinium (0.2 mmol/kg Magnevist,* 0.5 M)
Kurose et al. 2020[69]	'Healthy' LA wall	>2 SDs above the mean of "healthy" LA wall	1.5 T, 15 min post gadolinium (0.1 mmol/kg Gadovist, 1.0 M)
Ventricular Lesion Assessment			
Cochet et al. 2013[58]	Maximal myocardial signal	35–50% (BZ) or >50% (scar) of maximal signal intensity	1.5 T, 15 min post gadolinium (0.2 mmol/kg Dotarem, 0.5 M)
Fernandez-Armenta et al. 2013[57]	Maximal myocardial signal	40–60% (BZ) or >60% (scar) of maximal signal intensity	1.5 and 3 T, 7–10 min post gadolinium (0.2 mmol/kg Omniscan [GE Healthcare],* 0.5 M)
Yan et al. 2006[53]	Remote (healthy) myocardial segment	2–3 SDs (BZ) or >3 SDs (scar) above remote myocardium	1.5 T, 10–15 min post gadolinium (0.15–0.2 mmol/kg Magnevist,* 0.5 M)

*Authorisation of these linear gadolinium-based contrast agents for cardiac MRI has been suspended in the EU. †Mean of 'normal' indicates the average signal intensity of this area. BZ = border zone; IIR = image intensity ratio (the ratio between the signal intensity of each single pixel and the mean LA blood pool intensity for each patient); LA = left atrium.

RF-ablation-induced scar formation appear to apply similarly to cryoablation, albeit less well established and with an arguably more preserved ultrastructural tissue integrity.[27,28]

It has been shown that scar formation and remodelling in response to MI is a dynamic and chronically sustained process that continues over years after the initial injury.[29,30] Once recruited to injured myocardium, fibroblasts persist in the infarct scar for years where they continue to generate fibrogenic signals that perpetuate tissue repair and promote fibrosis.[29,30] While data from long-term longitudinal studies on ablation-induced scarring are lacking, a recent analysis of post-mortem cardiac samples from patients with previous ventricular tachycardia (VT) ablation, indicates that we have to consider such long-term remodelling processes also in response to catheter ablation.[25]

LGE-MRI for the Detection of Ablation-induced Fibrosis
Basic Principles
LGE-MRI for the detection of myocardial fibrosis was first used and histologically validated in a canine model of MI.[31] Despite pathophysiological differences, both cardiac ablation and MI result in coagulation necrosis, loss of syncytial membrane integrity and eventually replacement fibrosis. LGE-MRI makes use of the expansion of extracellular space and thus increased volume of distribution for the contrast agent that is associated with replacement fibrosis, as well as the prolonged washout owing to decreased capillary density within the myocardial fibrotic tissue.[32,33] Gadolinium-based contrast agents diffuse freely into the interstitium, but they cannot cross intact cell membranes and thus accumulate in the extracellular space. As gadolinium contrast agents

reduce the T1 relaxation time of adjacent tissue, LGE enhancement results in an increased signal intensity in T1-weighted MRI sequences. It is noteworthy though that LGE is not specific for fibrotic tissue, but can reflect other pathological processes associated with an expansion of the extracellular space such as inflammation and oedema formation, which impedes definite lesion assessment, particularly in the acute setting.[34]

Timing of Gadolinium Application
As indicated above, besides interstitial volume of distribution, LGE is determined by wash-in and washout kinetics of the contrast agent. Thus, the exact time delay between contrast administration and image acquisition is critical. While image acquisition is typically performed 7–15 minutes (ventricle) or 15–25 minutes (atrium) post contrast agent injection for differential spatial contrast between scar and normal tissue, there is no consensus among different centres. Moreover, in some cases the time delay may even be adapted, based on individual perfusion (cardiovascular function) and washout kinetics (renal function). At our centre, we acquire atrial images 20 minutes after an intravenous bolus of 0.2 mmol/kg of gadobutrol, whereas in the ventricle we acquire images 7–10 minutes after gadolinium injection.

Of note, the time to allow for gadolinium to enter lesions appears to be of particular relevance regarding the so-called dark core phenomenon. This phenomenon is characterised by a hypoenhanced region (dark core) within ablation lesions surrounded by a peripheral rim of LGE.[11,15,16,35] The exact pathological correlate underlying this phenomenon remains unknown, but microvascular obstruction impeding gadolinium wash-in is likely to play a role (no reflow). Possibly owing to a lack of functional capillaries, gadolinium appears to enter ablation lesions via diffusion from

the lesion periphery.[9,11] This hypothesis is based on the centripetal expansion of LGE towards the lesion centre resulting in a diminishment of the hypoenhanced dark core, which is observed with increasing time delays between gadolinium administration and image acquisition allowing for longer diffusion times.[9,11]

Contrast Agent and Dosage

The impact of different gadolinium-based contrast agents and doses on image quality are of particular interest in light of the recent safety concerns, not only regarding the induction of nephrogenic systemic fibrosis but also with respect to cerebral gadolinium deposits, the long-term clinical relevance of which is still unknown. Against this background, there may be a rationale to reduce doses of gadolinium-based contrast agents. While there has been no head-to-head-comparison of the different agents in the context of cardiac LGE imaging, recent data showed that Gadovist (Bayer) at 0.10 mmol/kg provides inferior LGE image quality than 0.15 and 0.20 mmol/kg with respect to ventricular scar assessment (image acquisition at a median of 9 minutes post gadolinium injection).[36] Interestingly, there is evidence suggesting that scans with 3T provide a signal-to-noise ratio that allows for better delineation of scarred myocardium than 1.5 T scans, even with lower contrast concentration (0.10 versus 0.20 mmol/kg Dotarem [Guerbet]), but again, systematic comparative data are lacking.[37]

While the above-mentioned results obtained for Gadovist and Dotarem, respectively, may not be generalisable to other gadolinium-based contrast agents, it has to be noted that, of the contrast agents presented in this review, only Gadovist and Dotarem are authorised for cardiac MRI in the EU (*Table 1*).

Image Acquisition

While several protocols have been detailed and validated previously, to date no consensus has been reached regarding standardised image acquisition and magnetic resonance (MR) sequence.[9,38–40] Typically 1.5 or 3 T scanners are used for post-contrast image acquisition employing fast 3D gradient echo sequences with ECG-gating and fat suppression. Low flip angles are applied to reduce saturation effects with short repetition times. To further optimise T1 contrast and signal intensities, inversion recovery sequences nullifying the signal of healthy ventricular myocardium are employed. Here, the optimum inversion time (TI) suppressing healthy myocardium (typically 250–300 ms) is determined empirically using a TI scout module prior to the acquisition of definite images. Healthy myocardium will thus appear hypoenhanced relative to scar tissue. TI values may have to be adapted during the scan to accommodate incremental T1 values of the normal myocardium owed to gadolinium washout.

To minimise cardiac motion artefacts, ECG gating is usually performed with the image acquisition window limited to <20% of the RR interval (typically 150–200 ms) and a trigger delay corresponding to atrial or ventricular mid-diastole, sparing atrial and ventricular contraction, respectively. In tachyarrhythmic patients, the trigger delay can be adapted according to the mean RR interval. However, we and others found signal-to-noise ratios substantially reduced in patients with AF.[39,41] Therefore, we strongly recommend cardioverting patients prior to the LGE-MRI study to avoid insufficient image quality. Long breath-holds required for image acquisition may be a limiting factor in some patients, a problem that is addressed by free-breathing 3D navigators that suppress respiratory motion artefacts through respiratory gating. Typical LGE-MRI sequences result in a voxel size of 1.25 x 1.25 x 2.5 mm with scan times of 10–15 minutes, depending on heart rate and breathing patterns.

The use of cardiac MRI in patients with implanted cardiac devices has been limited not only because of safety concerns, but also due to hyperintense image artefacts. While numerous studies and the advent of MR conditional cardiac pacemakers and ICDs have largely dispelled the safety concerns, image artefacts have remained a major limitation.[42–44] The artefacts are the result of significant distortion of the MRI magnetic field induced by the metallic pacemaker or ICD components.[45,46] They are typically located in the proximity (5–10 cm) of the device, with the distance being inversely associated with artefact size.[45,46] Of note, the artefacts are particularly pronounced in LGE-MRI sequences as applied for ablation lesion assessment. The use of lower magnetic field strength and shorter echo times has been shown to reduce artefacts, but this may be at the cost of image signal intensity and contrast.[46] Recently, based on the hypothesis that the device-related artefacts are caused by the limited spectral bandwidth of the inversion pulse that is typically applied in LGE-MRI, specific wideband MR sequences have been established.[47,48] We and other centres are now successfully employing these sequences, enabling high image quality without hyperintensity artefacts, even in the proximity of implanted devices.[49]

Image Post-processing

Several established open-source and commercial platforms for image post-processing are available. Most of these enable semiautomatic segmentation where manual tracings of the endocardial and/or epicardial borders are automatically adjusted to build a 3D anatomical shell. Relative signal intensities are then colour-coded and projected onto the 3D anatomical shell to create a relative LGE map discriminating healthy myocardium from scar tissue based on predefined thresholds. Some post-processing software even allows for integration of LGE maps into common electroanatomical mapping (EAM) systems.

As mentioned above, to date there is no standardised method for LGE image acquisition, and the same applies to image post-processing and analysis, which may explain the limited reproducibility across different centres. Most importantly, as T1-weighted imaging is based on signal intensity contrast rather than directly measured absolute values, LGE quantification requires a consistent internal reference for normalisation as well as validated signal intensity thresholds discriminating healthy and scar tissue.

While methods using normalisation based on the somewhat arbitrary definition of healthy atrial myocardium have been described for atrial lesion assessment, we and others use the mean signal intensity of the blood pool as an internal reference. Our group has recently established a method quantifying signal intensity ratios using the mean signal intensity of the left atrial (LA) blood pool as a reference (signal intensity of each given voxel/mean signal intensity of the blood).[38] Thresholds to define healthy myocardium (signal intensity ratio ≤1.2) and ablation-induced scarring (signal intensity ratio >1.32) in the atrium were derived from distinct cohorts of young healthy individuals as well as post-AF ablation patients, respectively, and subsequently validated in numerous clinical studies with respect to electroanatomical voltage mapping as well as clinical endpoints.[5–7] However, it should be emphasised that various other methods using distinct internal references and thresholds have been validated (*Table 1*).[17,39,50,51]

For ventricular lesion assessment the 'full width half maximum' method is the most commonly used approach, although other methods defining remote 'healthy' myocardial segments as an internal reference for normalisation have been described.[52–55] We found that the best agreement

Figure 1: Ablation-induced Late Gadolinium Enhancement After Pulmonary Vein Isolation
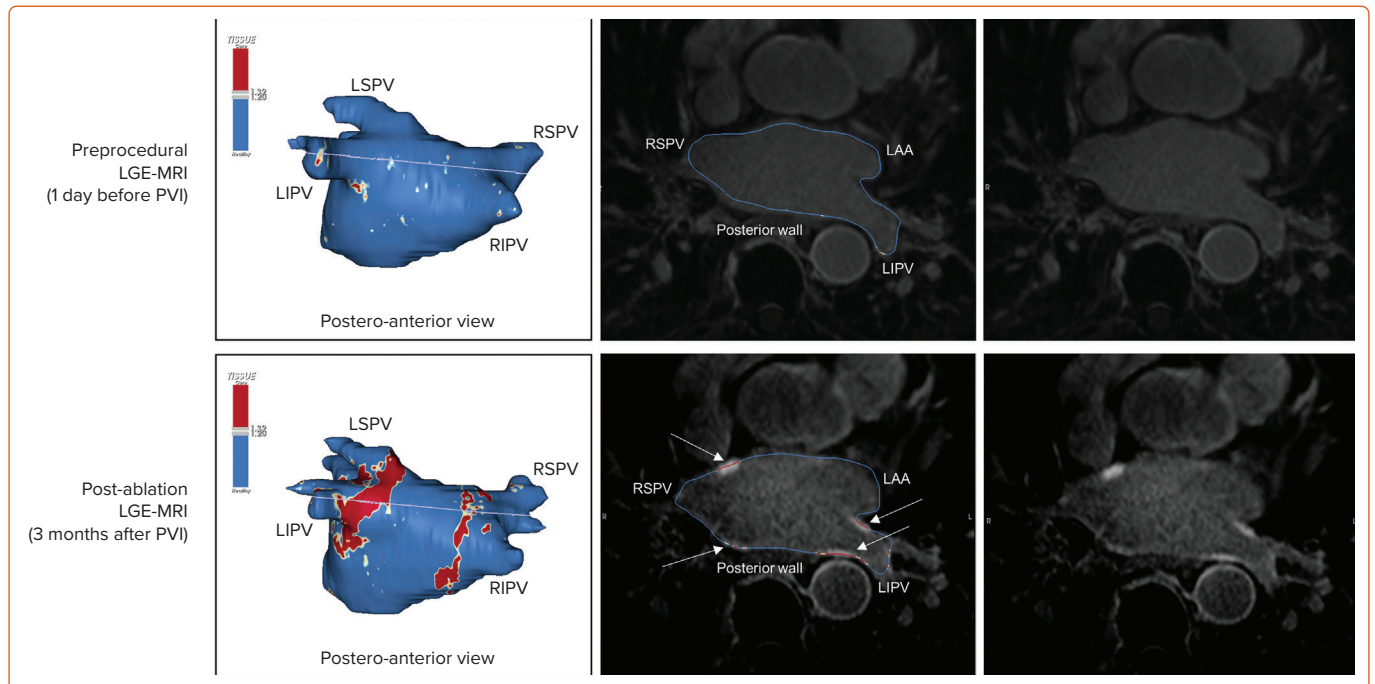
Left: 3D reconstruction of the LA with colour-coding based on image intensity ratios with thresholds for dense scar (red >1.32) and border zone (yellow 1.2–1.32), using ADAS 3D software (Adas3D Medical). Blue lines indicate the plane of the LA slices on the right. Middle: Overlay of the T1-weighted images with the LGE colour-coding described above. White arrows point to local ablation-induced LGE lesions. Right: T1-weighted LGE-MRI slice depicting the LA with evident LGE of PV ostial walls. LA = left atrium; LAA = left atrial appendage; LGE = late gadolinium enhancement; LIPV = left inferior pulmonary vein; LSPV = left superior pulmonary vein; PV = pulmonary vein; PVI = pulmonary vein isolation; RIPV = right inferior pulmonary vein; RSPV = right superior pulmonary vein.

with electroanatomical voltage mapping was achieved when applying thresholds of >60% (dense scar) and <40% (healthy tissue) of the maximum signal intensity, but again, other thresholds have been proposed too (*Table 1*).[56–59]

Timing of Lesion Assessment

As outlined above, we have to assume that ablation lesion formation is a dynamic process of sustained remodelling, which implies constant changes affecting cellular composition, extracellular space, water content and vascularisation, as well as small-vessel permeability and patency and intravascular pressure. These changes in turn, inevitably alter tissue-inherent magnetic properties and wash-in/washout kinetics of gadolium.[60,61] In fact, we found determination of definite atrial ablation lesions by LGE-MRI to be more accurate at 3 months post ablation than at later time points >12 months after ablation.[20] Thus, it is evident that lesion assessment by LGE-MRI is dependent on the exact time point. Moreover, LGE is not specific for fibrosis and does not necessarily indicate formation of durable ablation lesions. In fact, particularly in the acute setting, LGE may represent oedema reflecting a transient inflammatory response, which usually resolves within the first month following ablation.[11,62] In addition, the sensitivity of LGE to detect acute ablation lesions may be locally reduced by the above-mentioned dark core or no reflow phenomena, where limited diffusion times result in central hypoenhanced regions within ablation lesions. As diffusion distances are minimal in the thin-walled atrium, this phenomenon seems to be less relevant in the context of atrial ablation, where central hypoenhanced regions have only been observed in acute lesions.[35] Even in the ventricle, these hypoenhanced regions are less frequently encountered in chronic lesions >1 month post-ablation, possibly because of on-going remodelling of scar tissue including neovascularisation, although data are somewhat conflicting in this regard (see the section Ventricular Ablation Lesions, below).[11,15,16,63]

Taken together, these time-dependent limitations may argue for a late timing of LGE-MRI-based lesion assessment. However, we have recently found a decreased detectability of atrial ablation lesions at very late time-points, >12 months post-ablation, compared with an assessment at 3 months post ablation.[20] The long-term decrease in LGE of pulmonary vein (PV)-encircling ablation lesions observed in this study could in theory also reflect true regression of ablation-induced fibrosis; in fact, such a phenomenon has been proposed previously as a possible explanation for non-durable ablation lesions and late AF recurrences. However, using invasive high-density mapping as a reference, we found the decrease in LGE over time to be because of reduced detectability of ablation-induced fibrosis by LGE-MRI at time-points >12 months post ablation. Again, the pathological correlate underlying this observation is unclear, but likely to involve on-going remodelling altering tissue-inherent magnetic properties and wash-in/washout kinetics of the gadolinium contrast agent.

Against this background, the time-point of 3 months post ablation that has become an established standard for lesion assessment with LGE-MRI in many labs, appears reasonable. This time-point has been shown to reliably indicate chronic lesion formation in the atrium and in the ventricle and has been rigorously validated with respect to functional gaps detected by EAM as well as clinical endpoints like AF recurrence.[6,62,64,65]

Atrial Ablation Lesions
LGE-MRI of the Atrium

While LGE-MRI is a well-established tool to aid or guide VT ablation, its usage for the assessment of fibrosis in the atrium is somewhat lagging behind. This is because of – in part – two reasons. Firstly, unlike the well-demarcated extensive post-MI scar, atrial fibrosis is typically less extensive and more diffuse. This renders detection difficult, as conventional T1-weighted MRI relies on differential spatial contrast between normal tissue on one side and abnormal tissue on the other side. Secondly, differentiation

## Figure 2: Gaps in Ablation Lesions After Pulmonary Vein Isolation
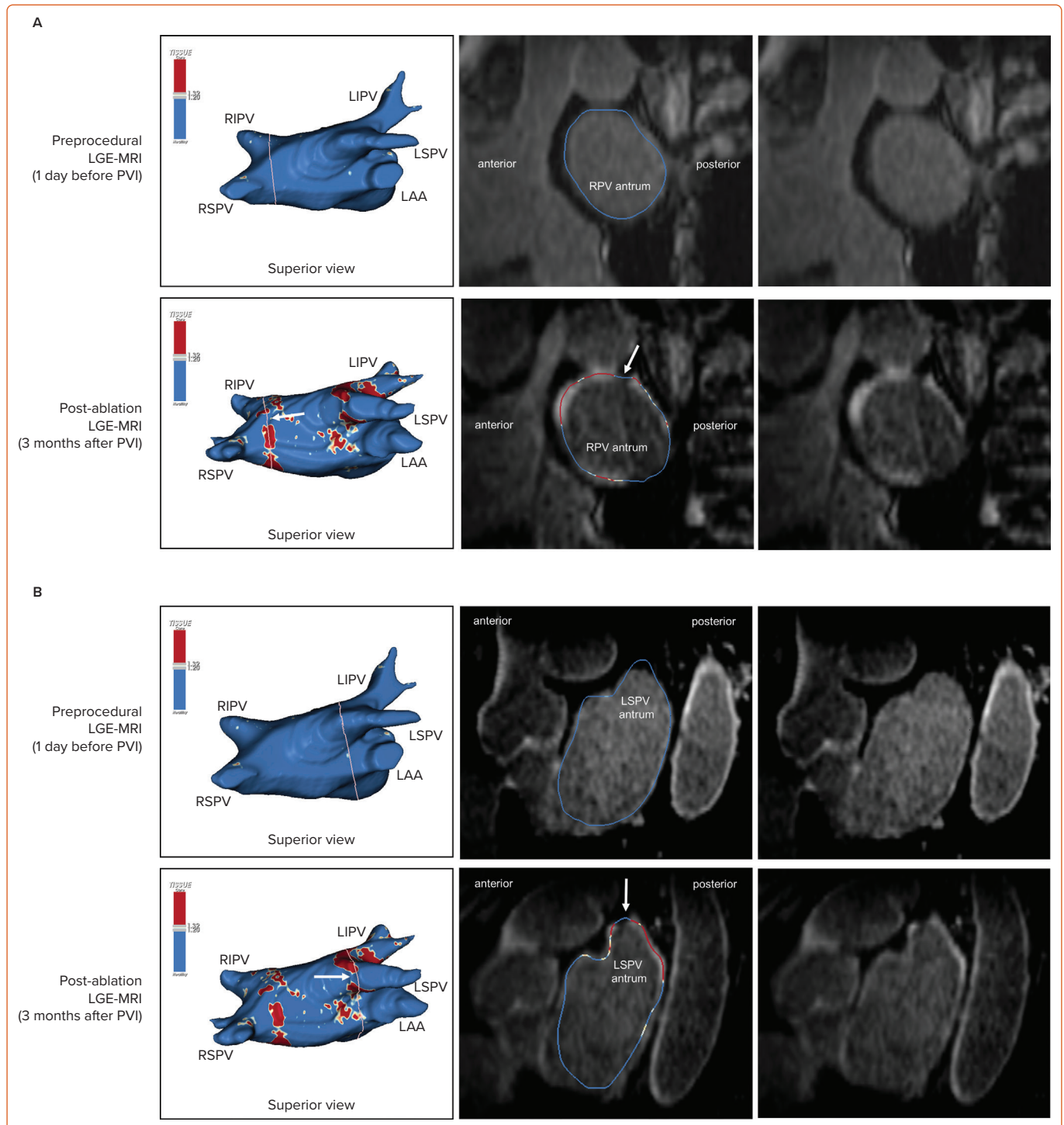
Examples of discontinuations of ablation-induced LGE lesions encircling the right (A) and left pulmonary veins (B), respectively, in a patient with AF recurrence after PVI. Left: 3D reconstruction of the LA with colour-coding based on image intensity ratios with thresholds for dense scar (red >1.32) and border zone (yellow 1.2–1.32), using ADAS 3D software). White arrows indicate local gaps. Pink lines indicate the plane of the left atrial LGE-MRI slices on the right; Middle: Overlay of the T1-weighted left atrial slices with the LGE colour-coding described above. White arrows indicate local gaps corresponding to the ones indicated in the 3D reconstructions on the left; Right: T1-weighted LGE-MRI slices without colour-coding. LA = left atrium; LAA = left atrial appendage; LGE = late gadolinium enhancement; LIPV = left inferior pulmonary vein; LSPV = left superior pulmonary vein; PV = pulmonary vein; PVI = pulmonary vein isolation; RPV = right pulmonary vein; RIPV = right inferior pulmonary vein; RSPV = right superior pulmonary vein.

of spatial contrast is particularly difficult in the thin-walled atrium with wall thicknesses down to 1 mm, which approximates the limit of spatial resolution of MRI. However, recent advances in MR imaging techniques, such as 3D navigated inversion recovery sequences, have yielded improved resolution and signal-to-noise ratios enabling valid tissue characterisation also in the atrium.[39,66] With respect to atrial ablation lesions it has to be considered that these constitute dense scar, which

facilitates discrimination from healthy tissue by LGE-MRI. Thus, even before validation of LGE-MRI for the detection of native atrial fibrosis, it was successfully employed for the assessment of atrial ablation-induced scarring (*Figure 1*).[40,64,67]

While initial studies evaluating the capability of LGE-MRI to accurately localise functional gaps within ablation lesions yielded conflicting results,

Figure 3: Agreement Between Electroanatomical Mapping and 3 Months Late Gadolinium Enhancement-MRI Regarding Gap Localisation

| LPV entry | RPV entry |
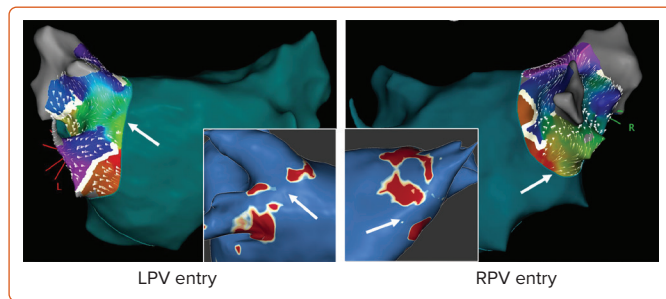
Activation maps of the LPVs and RPVs with conduction vectors (CARTO 3, coherent mapping with Pentaray catheter, Biosense Webster) indicating the entry site of the activation wave front (functional gaps) as detected during a repeat ablation procedure. Corresponding gaps detected by prior late gadolinium enhancement (LGE)-MRI (3 months post index ablation) are displayed in the small boxes. Colour-coding of the LGE maps (ADAS 3D software) is based on image intensity ratios with thresholds for dense scar (>1.32 red) and border zone (1.2–1.32 yellow), respectively. White arrows indicate localised functional gaps and LGE discontinuities, respectively. LPV = left pulmonary vein; RPV = right pulmonary vein.

depending on the performing centre, it has to be taken into account that time-points and protocols for image acquisition as well as post-processing methods varied substantially in these studies.[5,6,17,18] As outlined above, this may account for the lack of reproducibility. Promoted by further technological and methodological advances in the last decade, LGE-MRI is now being established as a useful standard for risk stratification, patient selection and lesion assessment in the context of AF ablation in a growing number of specialised centres.[2]

Of note, the feasibility of lesion assessment with LGE-MRI has been demonstrated, both in the context of RF ablation and cryoablation. Interestingly, apart from wider lesions observed after ablation with the cryoballoon compared with point-by-point RF ablation, both techniques result in quite similar LGE lesion characteristics.[68,69]

Non-invasive Confirmation of Durable PVI

Most importantly, LGE-MRI can non-invasively evaluate and confirm durable PVI and may thus replace invasive repeat procedures confirming PVI. Today, it is a common practice that symptomatic recurrences beyond the 3 months post-ablation blanking period almost automatically trigger a repeat procedure. However, to an increasing degree, all four PVs are found isolated in those repeat procedures. As ablation of extra-PV targets has failed to show benefit in large randomised trials, more and more often we may end up performing these highly invasive procedures only to confirm durable PVI; or even worse, investigators might feel obliged to ablate extra-PV targets to justify the invasive procedure. Against this background it is noteworthy that LGE-MRI has been shown to be capable of reliably confirming durable PVI with positive predictive values approaching 100%.[64] This is consistent with our experience where a complete circumferential LGE lesion set practically rules out PV reconnection. Thus, in patients with circumferential LGE lesions indicating durable PVI, there is no rationale for a repeat procedure, unless one is determined to target extra-PV structures (*Figure 1*).

However, it should be noted that in earlier studies, complete LGE lesions encircling all four PV were encountered only in around 7–28% of the repeat procedures.[64,70] Although we have to assume that these numbers have increased with recent advances in ablation techniques, in our experience the majority of patients still display discontinuities in the LGE lesions (*Figure 2*).

LGE-MRI-guided Repeat Ablation

Accumulating evidence indicates that LGE-MRI can detect and localise the gaps in ablation lesions with high accuracy (*Figure 3*).[5–7,14] Overall, the accuracy and in particular the high sensitivity in the detection of gaps appears to be sufficient for LGE-MRI-guided repeat ablation – not only in the context of AF (*Figure 4*), but also with respect to post-ablation reentrant atrial arrhythmias (*Figure 5*).[5,7,14]

Bisbal et al. were the first to demonstrate the feasibility of a merely LGE-MRI-guided approach in repeat PVI procedures.[5] They performed re-ablation based on a 3D reconstruction of the atrial LGE-MRI, which was integrated and merged into the EAM system, with the investigator blinded to any electrical information. A total of 15 patients underwent this LGE-MRI-guided approach, with re-isolation being accomplished in 95.6% of the reconnected PVs. In a subsequent study, the same approach even proved superior to segmental PV re-isolation based on electrical signals.[7] However, it has to be taken into account that this was not a randomised trial, but a case–control study with all its potential bias and limitations.

One possible explanation of the putative superiority of the LGE-MRI-guided approach could be the higher sensitivity of LGE-MRI regarding the detection of gaps. As outlined above, the negative predictive value of LGE-MRI to rule out gaps is very high.[20] However, gaps detected by LGE-MRI do not always correspond to a functional gap based on electrical signals. While this may reflect a limited specificity of LGE-MRI and failure to detect local ablation-induced scarring, it may in part be explained by a limited sensitivity of catheter-based gap detection, particularly when conventional catheters are used instead of microelectrode catheters. Moreover, LGE-MRI-determined anatomical gaps might colocalise with non-conductive tissue or a site of dormant conduction, rendering catheter-based gap detection impossible.

Taken together, the higher sensitivity of the LGE-MRI regarding the detection of gaps may be at the cost of specificity, but it is less likely that gaps are omitted. Thus, while segmental electrogram-guided repeat PVI might occasionally result in undertreatment, LGE-MRI potentially leads to a more complete re-ablation.

Incomplete lesion sets can also constitute an arrhythmogenic substrate for reentrant atrial tachycardias, which is more likely in the case of extensive ablation strategies. Fochler et al. recently showed that incomplete lesions and resulting isthmi can be detected by LGE-MRI. They found that a dechannelling approach targeting LGE-MRI-detected isthmi, analogously to VT substrate ablation strategies, may be feasible and appropriate as a standalone approach in patients with recurrent atrial tachycardias after initial AF ablation.[14]

## Lesion Assessment to Predict Ablation Outcome

Besides being a valuable tool for patient selection and guidance of repeat ablation procedures, LGE-MRI-based lesion assessment has yielded several predictors of AF recurrence, with the most obvious one being related to PV reconnection. Interestingly, Linhart et al. found LGE-MRI-detected gaps to predict AF recurrences, but it was not the presence of gaps *per se* or the number of gaps that predicted recurrences, but the cumulative length of all gaps added together relative to the circumference of ipsilateral PVs. In the 94 patients included in their study, the risk of recurrence increased by 16% with every 10% gap length relative to the PV-encircling ablation line. So, while a single small gap detected by LGE-MRI may not be critical with respect to outcome, extensive or multiple gaps are critical.[6]

Figure 4: Single-touch Late Gadolinium Enhancement-MRI-guided Repeat Pulmonary Vein Isolation
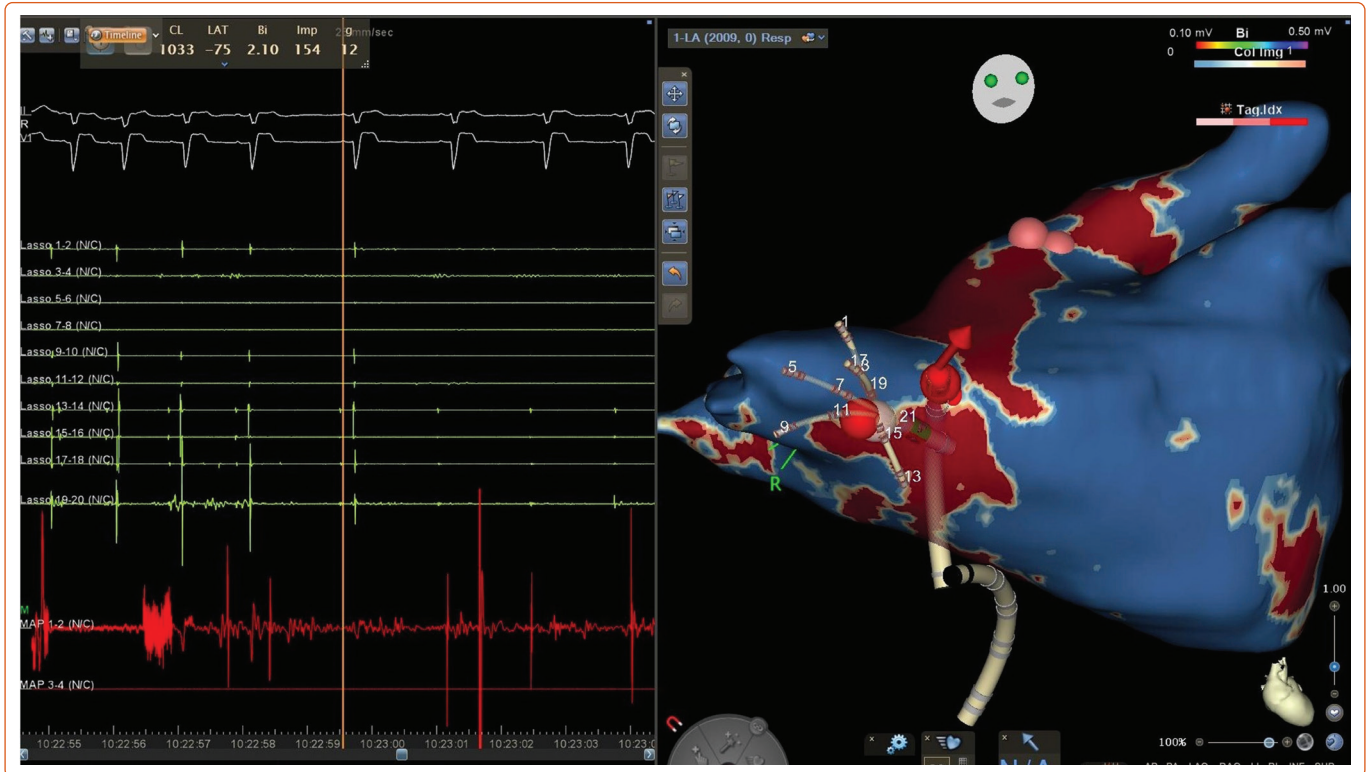
Late gadolinium enhancement (LGE) map (ADAS 3D software) integrated into the 3D mapping system (CARTO 3) for targeted ablation of a single LGE-discontinuity at the right superior pulmonary vein (PV) (right panel) resulting in immediate PV isolation upon radiofrequency application as reflected by the disappearance of the PV electrograms detected by the multipolar mapping catheter (Pentaray, Biosense Webster). Colour-coding of LGE map: Image intensity ratio thresholds for dense scar >1.32 (red) and border zone 1.2–1.32 (yellow).

Figure 5: Recurrent Perimitral Flutter After Two Mitral Isthmus Ablations
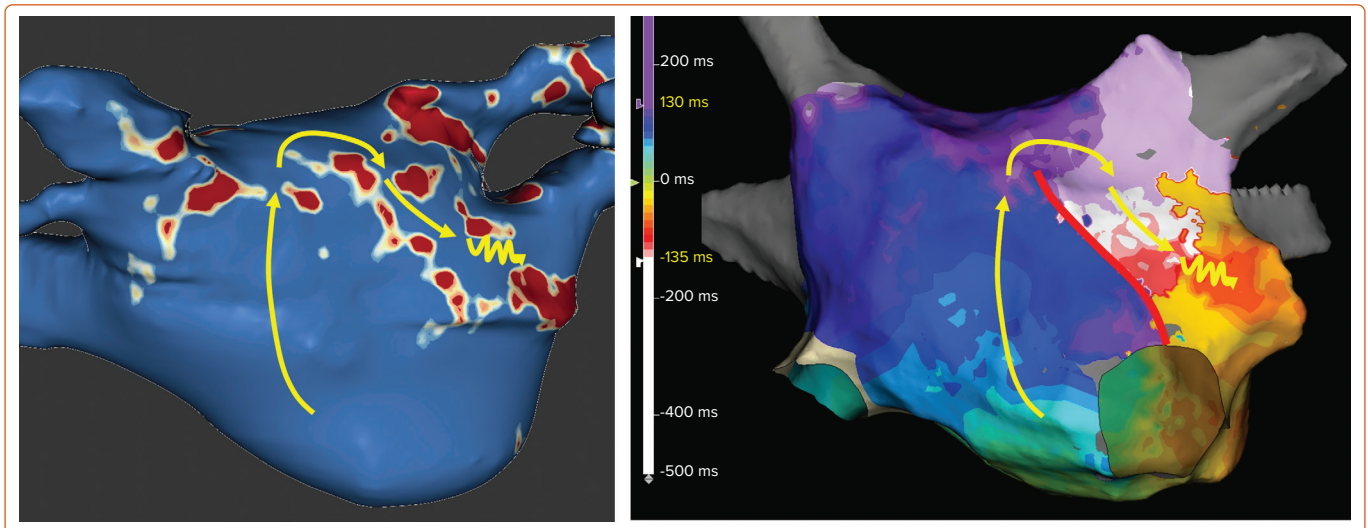

Left: Late gadolinium enhancement map of the left atrium (LA) 3 months post mitral isthmus re-ablation (ADAS 3D software). The impulse propagation as determined by electroanatomical mapping (activation mapping with HD grid and EnSite Precision [Abbott Medical]) during the repeat procedure is indicated by yellow arrows. These illustrate how lesions from previous ablations force the wave front to go around the LA roof before meandering back to the mitral isthmus through gaps in the ablation line. Dechannelling by ablating the critical isthmus of slow conduction terminated the tachycardia and rendered it non-inducible. Colour-coding of late gadolinium enhancement map: image intensity ratio thresholds for dense scar >1.32 (red) and border zone 1.2–1.32 (yellow). Right: LA activation during flutter (mapping with HD grid and EnSite Precision). Yellow arrows indicate impulse propagation. Line of conduction block illustrated by red line.

These data are in line with a study by Akoum et al. using LGE-MRI before and 3 months after AF ablation to evaluate ablation lesions and modification of potentially arrhythmogenic substrate.[71] They also found the presence of LGE-MRI-detected gaps in PV encircling ablation lines *per se* not to be predictive of recurrences. However, besides LGE-MRI-detected baseline atrial fibrosis, they identified residual fibrosis, i.e. fibrotic area not homogenised by ablation, as a predictor of AF recurrence.

Recent work by Kamali et al. assessed ablation lesions and their potential barrier function for electrical propagation in persistent AF.[72] They identified the atrial area available for AF to propagate, as determined by LGE-MRI,

Figure 6: Ventricular Ablation Lesion Assessment
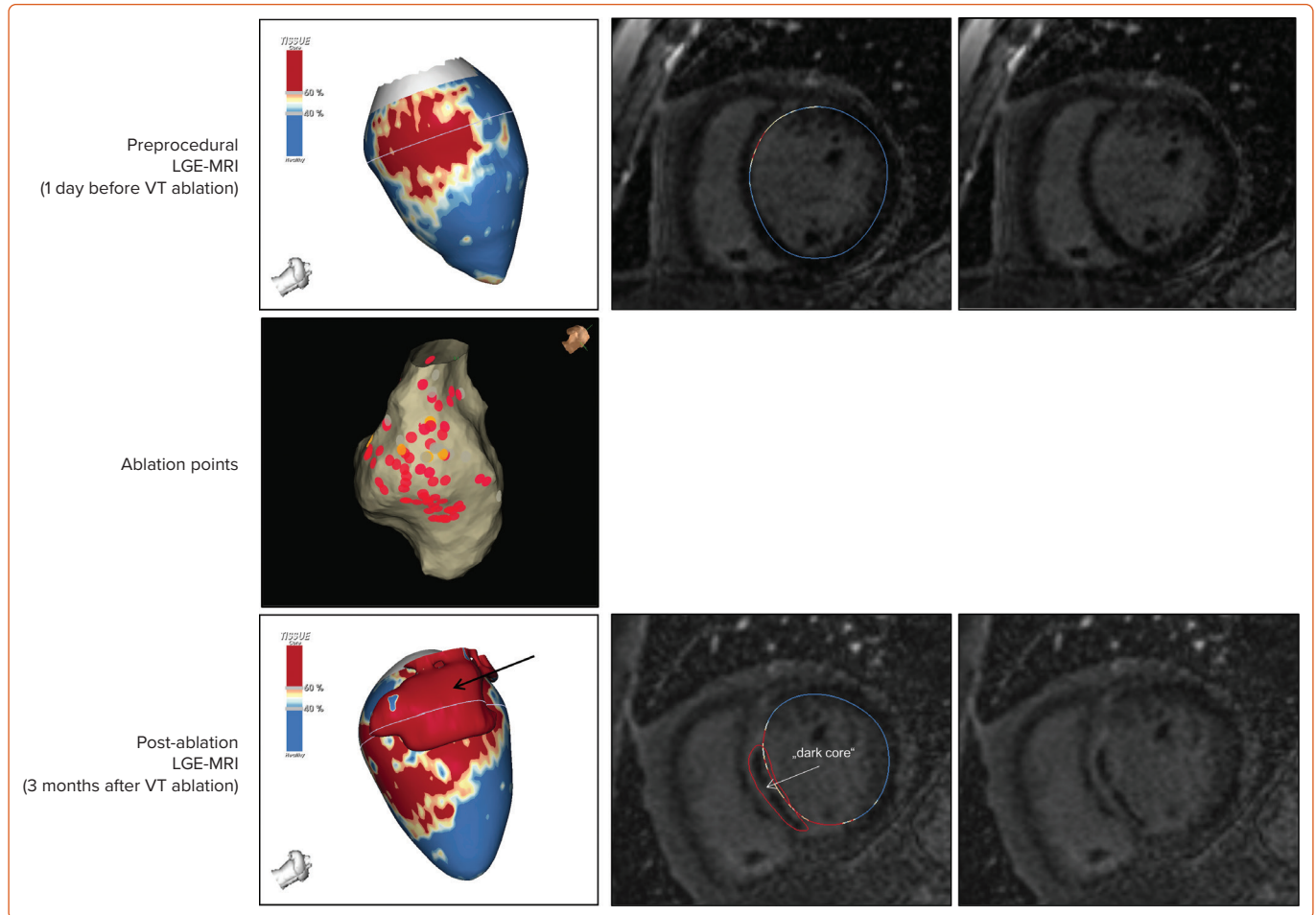
Left: 3D reconstruction of the left ventricle with LGE-based colour-coding based on thresholds for dense scar (red, >60% maximum of signal intensity) and border zone (yellow, 40–60% of maximum signal intensity), mapped using ADAS 3D. Shown are the layers at 30% of the transmurality (from endocardial to epicardial). For the post-ablation LGE-MRI (lower panel), an additional 3D reconstruction of the manually defined dark core in red (black arrow) is depicted. Blue lines indicate the plane of the short-axis slices on the right. The ablation points (TactiCath, Abbott Medical) are visualised using a 3D mapping system (EnSite Precision, Abbott Medical). Middle: Overlay of the T1-weighted short-axis slices with the colour-coding described above. The central hypoenhancement dark core of the ablation lesion is manually delineated (red border) to avoid misinterpretation as healthy tissue. Right: T1-weighted short-axis LGE-MRI slices without colour-coding. LGE = late gadolinium enhancement; VT = ventricular tachycardia.

as a predictor of recurrence after catheter ablation. Interestingly, this variable predicted recurrences better than did established predictors such as LA volume or total atrial fibrosis.

Ventricular Ablation Lesions
Objective of Lesion Assessment in the Ventricle
Even though LGE-MRI was first established for ventricular tissue characterisation and is by now widely used as a clinical tool to guide VT ablation through detection of arrhythmogenic substrate, there has been less interest in ablation lesion assessment in the ventricle than the atrium. This may be because of the fact that ablation strategies, and thus requirements for non-invasive ablation lesion assessment, are fundamentally different in the ventricle compared to the atrium. While in the atrium continuity and transmurality of predefined lesion sets are assessed, in the ventricle the endpoint is rather elimination or modification of arrhythmogenic substrate. The capability of LGE-MRI to accurately localise arrhythmogenic substrate in terms of scar border zone and slow conduction channels in a 3D fashion is meanwhile well-established; this is also true for patients with implanted cardiac devices when employing specific wideband MRI sequences.[4,49,56,57,73–75] However, the elimination of LGE-MRI-detected arrhythmogenic substrate as a potential endpoint of VT ablation has not been studied.

Feasibility of Ventricular Lesion Assessment
Several preclinical and few early observational clinical studies evaluated the feasibility of LGE-MRI for ventricular ablation lesion assessment. Most of these studies investigated lesion formation in the acute setting, at time points when reliable discrimination of irreversible lesions from transient oedema based on LGE is highly challenging, if not impossible.[9,12,76–78] While oedema has been demonstrated to resolve within 1–2 weeks from ablation, formation of definite lesions appears to take up to 8 weeks.[10,11,25] Of note, Yamashita et al. demonstrated strong correlation of depth and volume of LGE lesions with definite lesions as determined by gross pathology in a canine model 8 weeks after ablation.[10]

Studies in patients with idiopathic and ischaemic VT have demonstrated that these definite ablation lesions can be visualised by LGE-MRI even many months after the ablation.[15,16]

The Dark Core Phenomenon
For image post-processing and analyses it has to be taken into account that, in contrast to atrial ablation lesions, the above-mentioned dark core phenomenon, characterised by centrally hypoenhanced lesions, has been observed even in these chronic stages of ventricular lesion formation, thus complicating the assessment of ablation-induced scarring

Figure 7: Assessing Elimination of Arrhythmogenic Fibrotic Substrate by Late Gadolinium Enhancement-MRI
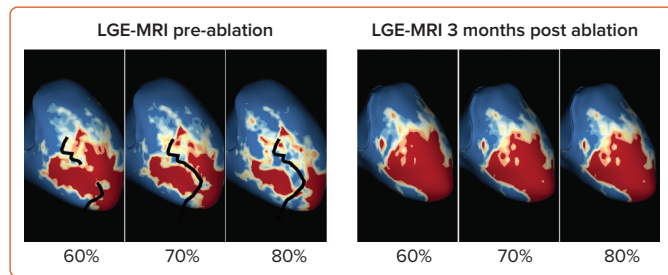
Left panel: LGE map of the left ventricle prior to substrate-based ventricular tachycardia ablation. LGE depicts an antero-apical scar. A 3D-analysis using the ADAS 3D software predicts a slow-conduction channel (black line) extending over 30 % of the transmurality that was confirmed by invasive electroanatomical mapping. Right panel: LGE map of the left ventricle 3 months post-ventricular tachycardia ablation. LGE indicates complete scar homogenisation and 'dechannelling' with ablation lesions covering the full substrate. Percentages indicate distinct layers of the transmurality from endocardial (0%) to epicardial (100%). LGE = late gadolinium enhancement.

in the ventricle.[15] As current post-processing software algorithms are solely based on hyperenhancement, hypoenhanced lesion cores are not automatically identified and thus have to be delineated manually to avoid misinterpretation (*Figure 6*).

While Vunnam et al. have recently reported to have found 'dark core' lesions only up to 1 month after RF ablation but not at later stages, which is in line with previous preclinical and clinical data, Dabbagh et al. consistently observed lesions with hypoenhanced cores as late as 30 months post-ablation in all patients after repeat ablation of post-MI substrates.[11,15,16,63] Of note, at our centre, we encounter centrally hypoenhanced lesions in around 60% of the patients at the systematic follow-up LGE-MRI 3–6 months post-VT ablation. Interestingly, in the study of Vunnam et al., comparison with pre-procedural LGE-MRI scans revealed that dark core lesions could only be observed in previously non-fibrotic myocardium without preexisting scar, suggesting that different wash-in/washout kinetics in scarred versus non-scarred myocardium play a role in this context. This is in line with a study in patients devoid of structural heart disease in whom LGE-MRI was performed at a mean of 22 months after ablation of idiopathic VT, where no central hypoenhancement of lesions was encountered.[16]

Potential Clinical Value of Ventricular Lesion Assessment

While cumulative evidence is suggesting feasibility of LGE-MRI-based ventricular ablation lesion assessment, clinical validation is absent.

Against this background, we have recently analysed the potential role of LGE-MRI to assess the long-term effect of VT ablation in terms of arrhythmogenic substrate elimination (unpublished data). Three to 6 months following the procedure, effective ablation was reflected by pronounced reduction of LGE-MRI-detected border zone scar volume and extent of slow conduction channels compared to the preprocedural LGE-MRI (*Figure 7*). In patients undergoing repeat ablation procedures, this arrhythmogenic substrate elimination as determined by LGE-MRI correlated well with EAM. Thus, LGE-MRI-based lesion assessment may be of potential value to evaluate the efficacy of ventricular substrate ablation and to predict VT recurrences and clinical outcome. However, as mentioned above, clinical validation is warranted.

Conclusion

LGE-MRI constitutes the gold standard for non-invasive ablation lesion assessment. In the context of atrial ablation, LGE-MRI-based lesion assessment is already employed in routine clinical settings for non-invasive confirmation of durable PVI and to guide repeat ablation procedures in selected centres. In contrast, ventricular lesion assessment by LGE-MRI is less well established. However, despite the lack of clinical validation, LGE-MRI-based evaluation of arrhythmogenic substrate elimination holds great promise as an efficacy endpoint for VT ablation and a potential predictor of recurrences and clinical outcome.

In light of the current limitations, there is clearly some work ahead of us. Most importantly, uniform methodological and analytical standards are warranted to increase reproducibility of results across centres. This in turn, will foster the acceptance of the method and a broader implementation into clinical practice. ❏

Clinical Perspective

- Late-gadolinium-enhancement (LGE)-MRI offers the unique capability of non-invasive ablation lesion assessment.
- LGE-MRI can detect and localise functional gaps in atrial lesion sets with high accuracy, which also allows for MRI-guided repeat ablation.
- Because of a very high negative predictive value regarding the detection of functional gaps, LGE-MRI can reliably rule out pulmonary vein reconnection non-invasively and may thus avoid unnecessary invasive repeat procedures where a pulmonary-vein-isolation-only approach is pursued.
- Elimination of LGE-MRI-detected arrhythmogenic substrate may serve as a potential efficacy endpoint and predictor of clinical outcomes in ventricular tachycardia ablation.

1. Pontecorboli G, Figueras I Ventura RM, Carlosena A, et al. Use of delayed-enhancement magnetic resonance imaging for fibrosis detection in the atria: a review. *Europace* 2017;19:180–9. https://doi.org/10.1093/europace/euw053; PMID: 28172967.
2. Hindricks G, Potpara T, Dagres N, et al. ESC guidelines for the diagnosis and management of atrial fibrillation developed in collaboration with the European Association of Cardio-Thoracic Surgery (EACTS). *Eur Heart J* 2021;42:373–498. https://doi.org/10.1093/eurheartj/ehaa612; PMID: 32860505.
3. Cronin EM, Bogun FM, Maury P, et al. 2019 HRS/EHRA/APHRS/LAHRS expert consensus statement on catheter ablation of ventricular arrhythmias: executive summary. *Europace* 2020;22:450–95. https://doi.org/10.1093/europace/euz332; PMID: 31995197.
4. Berruezo A, Penela D, Jáuregui B, Soto-Iglesias D. The role of imaging in catheter ablation of ventricular arrhythmias.

Pacing Clin Electrophysiol 2021;44:1115–25. https://doi.org/10.1111/pace.14183; PMID: 33527461.
5. Bisbal F, Guiu E, Cabanas-Grandio P, et al. CMR-guided approach to localize and ablate gaps in repeat AF ablation procedure. *JACC Cardiovasc Imaging* 2014;7:653–63. https://doi.org/10.1016/j.jcmg.2014.01.014; PMID: 24813966.
6. Linhart M, Alarcon F, Borras R, et al. Delayed gadolinium enhancement magnetic resonance imaging detected anatomic gap length in wide circumferential pulmonary vein ablation lesions is associated with recurrence of atrial fibrillation. *Circ Arrhythm Electrophysiol* 2018;11:e006659. https://doi.org/10.1161/CIRCEP.118.006659; PMID: 30562102.
7. Quinto L, Cozzari J, Benito E, et al. Magnetic resonance-guided re-ablation for atrial fibrillation is associated with a lower recurrence rate: a case-control study. *Europace* 2020;22:1805–11. https://doi.org/10.1093/europace/euaa252; PMID: 33063124.
8. Chubb H, Aziz S, Karim R, et al. Optimization of late

gadolinium enhancement cardiovascular magnetic resonance imaging of post-ablation atrial scar: a cross-over study. *J Cardiovasc Magn Reson* 2018;20:30. https://doi.org/10.1186/s12968-018-0449-8; PMID: 29720202.
9. Dickfeld T, Kato R, Zviman M, et al. Characterization of radiofrequency ablation lesions with gadolinium-enhanced cardiovascular magnetic resonance imaging. *J Am Coll Cardiol* 2006;47:370–8. https://doi.org/10.1016/j.jacc.2005.07.070; PMID: 16412863.
10. Yamashita K, Kholmovski E, Ghafoori E, et al. Characterization of edema after cryo and radiofrequency ablations based on serial magnetic resonance imaging. *J Cardiovasc Electrophysiol* 2019;30:255–62. https://doi.org/10.1111/jce.13785; PMID: 30375090.
11. Ghafoori E, Kholmovski EG, Thomas S, et al. Characterization of gadolinium contrast enhancement of radiofrequency ablation lesions in predicting edema and chronic lesion size. *Circ Arrhythm Electrophysiol*

2017;10:e005599. https://doi.org/10.1161/CIRCEP.117.005599; PMID: 29079664.

12. Nordbeck P, Hiller KH, Fidler F, et al. Feasibility of contrast-enhanced and nonenhanced MRI for intraprocedural and postprocedural lesion visualization in interventional electrophysiology: animal studies and early delineation of isthmus ablation lesions in patients with typical atrial flutter. *Circ Cardiovasc Imaging* 2011;4:282–94. https://doi.org/10.1161/CIRCIMAGING.110.957670; PMID: 21415125.

13. Spragg DD, Khurram I, Nazarian S. Role of magnetic resonance imaging of atrial fibrosis in atrial fibrillation ablation. *Arrhythm Electrophysiol Rev* 2013;2:124–7. https://doi.org/10.15420/aer.2013.2.2.124; PMID: 26835053.

14. Fochler F, Yamaguchi T, Kheirkahan M, et al. Late gadolinium enhancement magnetic resonance imaging guided treatment of post atrial fibrillation ablation recurrent arrhythmia. *Circ Arrhythm Electrophysiol* 2019;12:e007174. https://doi.org/10.1161/CIRCEP.119.007174; PMID: 31422685.

15. Dabbagh GS, Ghannam M, Siontis KC, et al. Magnetic resonance mapping of catheter ablation lesions after post-infarction ventricular tachycardia ablation. *JACC Cardiovasc Imaging* 2021;14:588–98. https://doi.org/10.1016/j.jcmg.2020.08.041; PMID: 33248970.

16. Ilg K, Baman TS, Gupta SK, et al. Assessment of radiofrequency ablation lesions by CMR imaging after ablation of idiopathic ventricular arrhythmias. *JACC Cardiovasc Imaging* 2010;3:278–85. https://doi.org/10.1016/j.jcmg.2009.09.028; PMID: 20223425.

17. Harrison JL, Sohns C, Linton NW, et al. Repeat left atrial catheter ablation: cardiac magnetic resonance prediction of endocardial voltage and gaps in ablation lesion sets. *Circ Arrhythm Electrophysiol* 2015;8:270–8. https://doi.org/10.1161/CIRCEP.114.002066; PMID: 25593109.

18. Spragg DD, Khurram I, Zimmerman SL, et al. Initial experience with magnetic resonance imaging of atrial scar and co-registration with electroanatomic voltage mapping during atrial fibrillation: success and limitations. *Heart Rhythm* 2012;9:2003–9. https://doi.org/10.1016/j.hrthm.2012.08.039; PMID: 23000671.

19. Mărgulescu AD, Nuñez-Garcia M, Alarcón F, et al. Reproducibility and accuracy of late gadolinium enhancement cardiac magnetic resonance measurements for the detection of left atrial fibrosis in patients undergoing atrial fibrillation ablation procedures. *Europace* 2019;21:724–31. https://doi.org/10.1093/europace/euy314; PMID: 30649273.

20. Althoff TF, Garre P, Caixal G, et al. Late gadolinium enhancement-MRI determines definite lesion formation most accurately at three months post ablation compared to later time points. *Pacing Clin Electrophysiol* 2022;45:72–82. https://doi.org/10.1111/pace.14415; PMID: 34820857.

21. Chubb H, Williams SE, Whitaker J, et al. Cardiac electrophysiology under MRI guidance: an emerging technology. *Arrhythm Electrophysiol Rev* 2017;6:85–93. https://doi.org/10.15420/aer.2017.1.2; PMID: 28845235.

22. Deneke T, Khargi K, Müller KM, et al. Histopathology of intraoperatively induced linear radiofrequency ablation lesions in patients with chronic atrial fibrillation. *Eur Heart J* 2005;26:1797–803. https://doi.org/10.1093/eurheartj/ehi255; PMID: 15855195.

23. Gepstein L, Hayam G, Shpun S, et al. Atrial linear ablations in pigs. Chronic effects on atrial electrophysiology and pathology. *Circulation* 1999;100:419–26. https://doi.org/10.1161/01.CIR.100.4.419; PMID: 10421604.

24. Harrison JL, Jensen HK, Peel SA, et al. Cardiac magnetic resonance and electroanatomical mapping of acute and chronic atrial ablation injury: a histological validation study. *Eur Heart J* 2014;35:1486–95. https://doi.org/10.1093/eurheartj/eht560; PMID: 24419806.

25. Glashan CA, Stevenson W, Zeppenfeld K. Lesion size and lesion maturation after radiofrequency catheter ablation for ventricular tachycardia in humans with nonischemic cardiomyopathy. *Circ Arrhythm Electrophysiol* 2021;14:e009808. https://doi.org/10.1161/CIRCEP.121.009808; PMID: 34397261.

26. Althoff TF, Mont L. Novel concepts in atrial fibrillation ablation-breaking the trade-off between efficacy and safety. *J Arrhythm* 2021;37:904–11. https://doi.org/10.1002/joa3.12592; PMID: 34386116.

27. Khairy P, Dubuc M. Transcatheter cryoablation part I: preclinical experience. *Pacing Clin Electrophysiol* 2008;31:112–20. https://doi.org/10.1111/j.1540-8159.2007.00934.x; PMID: 18181919.

28. Manasse E, Colombo P, Roncalli M, Gallotti R. Myocardial acute and chronic histological modifications induced by cryoablation. *Eur J Cardiothorac Surg* 2000;17:339–40. https://doi.org/10.1016/S1010-7940(99)00361-9; PMID: 10847689.

29. Rog-Zielinska EA, Norris RA, Kohl P, Markwald R. The living scar – cardiac fibroblasts and the injured heart. *Trends Mol Med* 2016;22:99–114. https://doi.org/10.1016/j.molmed.2015.12.006; PMID: 26776094.

30. Sun Y, Weber KT. Infarct scar: a dynamic tissue. *Cardiovasc Res* 2000;46:250–6. https://doi.org/10.1016/S0008-6363(00)00032-8; PMID: 10773228.

31. Kim RJ, Fieno DS, Parrish TB, et al. Relationship of MRI delayed contrast enhancement to irreversible injury, infarct age, and contractile function. *Circulation* 1999;100:1992–2002. https://doi.org/10.1161/01.CIR.100.19.1992; PMID: 10556226.

32. Bing R, Dweck MR. Myocardial fibrosis: why image, how to image and clinical implications. *Heart* 2019;105:1832–40. https://doi.org/10.1136/heartjnl-2019-315560; PMID: 31649047.

33. Mewton N, Liu CY, Croisille P, et al. Assessment of myocardial fibrosis with cardiovascular magnetic resonance. *J Am Coll Cardiol* 2011;57:891–903. https://doi.org/10.1016/j.jacc.2010.11.013; PMID: 21329834.

34. Kiuchi K, Fukuzawa K, Nogami M, et al. Visualization of intensive atrial inflammation and fibrosis after cryoballoon ablation: PET/MRI and LGE-MRI analysis. *J Arrhythm* 2021;37:52–9. https://doi.org/10.1002/joa3.12454; PMID: 33664886.

35. McGann C, Kholmovski E, Blauer J, et al. Dark regions of no-reflow on late gadolinium enhancement magnetic resonance imaging result in scar formation after atrial fibrillation ablation. *J Am Coll Cardiol* 2011;58:177–85. https://doi.org/10.1016/j.jacc.2011.04.008; PMID: 21718914.

36. Monti CB, Codari M, Cozzi A, et al. Image quality of late gadolinium enhancement in cardiac magnetic resonance with different doses of contrast material in patients with chronic myocardial infarction. *Eur Radiol Exp* 2020;4:21. https://doi.org/10.1186/s41747-020-00149-2; PMID: 32242266.

37. Lim J, Park EA, Song YS, Lee W. Single-dose gadoterate meglumine for 3T late gadolinium enhancement MRI for the assessment of chronic myocardial infarction: intra-individual comparison with conventional double-dose 1.5T MRI. *Korean J Radiol* 2018;19:372–80. https://doi.org/10.3348/kjr.2018.19.3.372; PMID: 29713214.

38. Benito EM, Carlosena-Remirez A, Guasch E, et al. Left atrial fibrosis quantification by late gadolinium-enhanced magnetic resonance: a new method to standardize the thresholds for reproducibility. *Europace* 2017;19:1272–9. https://doi.org/10.1093/europace/euw219; PMID: 27940935.

39. Oakes RS, Badger TJ, Kholmovski EG, et al. Detection and quantification of left atrial structural remodeling with delayed-enhancement magnetic resonance imaging in patients with atrial fibrillation. *Circulation* 2009;119:1758–67. https://doi.org/10.1161/CIRCULATIONAHA.108.811877; PMID: 19307477.

40. Peters DC, Wylie JV, Hauser TH, et al. Detection of pulmonary vein and left atrial scar after catheter ablation with three-dimensional navigator-gated delayed enhancement MR imaging: initial experience. *Radiology* 2007;243:690–5. https://doi.org/10.1148/radiol.2433060417; PMID: 17517928.

41. Vijayakumar S, Kholmovski E, McGann C, Marrouche NF. Dependence of contrast to noise ratio between ablation scar and other tissues on patient heart rate and flip angle for late gadolinium enhancement imaging of the left atrium. *J Cardiovasc Magn Reson* 2012;14(Suppl 1):o107. https://doi.org/10.1186/1532-429X-14-S1-O107.

42. Glikson M, Nielsen JC, Kronborg MB, et al. 2021 ESC guidelines on cardiac pacing and cardiac resynchronization therapy. *Eur Heart J* 2021;42:3427–520. https://doi.org/10.1093/eurheartj/ehab364; PMID: 34455430.

43. Indik JH, Gimbel JR, Abe H, et al. 2017 HRS expert consensus statement on magnetic resonance imaging and radiation exposure in patients with cardiovascular implantable electronic devices. *Heart Rhythm* 2017;14:e97–153. https://doi.org/10.1016/j.hrthm.2017.04.025; PMID: 28502708.

44. Nazarian S, Hansford R, Rahsepar AA, et al. Safety of magnetic resonance imaging in patients with cardiac devices. *N Engl J Med* 2017;377:2555–64. https://doi.org/10.1056/NEJMoa1604267; PMID: 29281579.

45. Dickfeld T, Tian J, Ahmad G, et al. MRI-guided ventricular tachycardia ablation: integration of late gadolinium-enhanced 3D scar in patients with implantable cardioverter-defibrillators. *Circ Arrhythm Electrophysiol* 2011;4:172–84. https://doi.org/10.1161/CIRCEP.110.958744; PMID: 21270103.

46. Sasaki T, Hansford R, Zviman MM, et al. Quantitative assessment of artifacts on cardiac magnetic resonance imaging of patients with pacemakers and implantable cardioverter-defibrillators. *Circ Cardiovasc Imaging* 2011;4:662–70. https://doi.org/10.1161/CIRCIMAGING.111.965764; PMID: 21946701.

47. Rashid S, Rapacchi S, Shivkumar K, et al. Modified wideband three-dimensional late gadolinium enhancement MRI for patients with implantable cardiac devices. *Magn Reson Med* 2016;75:572–84. https://doi.org/10.1002/mrm.25601; PMID: 25772155.

48. Rashid S, Rapacchi S, Vaseghi M, et al. Improved late gadolinium enhancement MR imaging for patients with implanted cardiac devices. *Radiology* 2014;270:269–74. https://doi.org/10.1148/radiol.13130942; PMID: 24086074.

49. Roca-Luque I, Van Breukelen A, Alarcon F, et al. Ventricular scar channel entrances identified by new wideband cardiac magnetic resonance sequence to guide ventricular tachycardia ablation in patients with cardiac defibrillators. *Europace* 2020;22:598–606. https://doi.org/10.1093/europace/euaa021; PMID: 32101605.

50. Khurram IM, Beinart R, Zipunnikov V, et al. Magnetic resonance image intensity ratio, a normalized measure to enable interpatient comparability of left atrial fibrosis. *Heart Rhythm* 2014;11:85–92. https://doi.org/10.1016/j.hrthm.2013.10.007; PMID: 24096166.

51. Jefairi NA, Camaioni C, Sridi S, et al. Relationship between atrial scar on cardiac magnetic resonance and pulmonary vein reconnection after catheter ablation for paroxysmal atrial fibrillation. *J Cardiovasc Electrophysiol* 2019;30:727–40. https://doi.org/10.1111/jce.13908; PMID: 30847990.

52. Amado LC, Gerber BL, Gupta SN, et al. Accurate and objective infarct sizing by contrast-enhanced magnetic resonance imaging in a canine myocardial infarction model. *J Am Coll Cardiol* 2004;44:2383–9. https://doi.org/10.1016/j.jacc.2004.09.020; PMID: 15607402.

53. Yan AT, Shayne AJ, Brown KA, et al. Characterization of the peri-infarct zone by contrast-enhanced cardiac magnetic resonance imaging is a powerful predictor of post-myocardial infarction mortality. *Circulation* 2006;114:32–9. https://doi.org/10.1161/CIRCULATIONAHA.106.613414; PMID: 16801462.

54. Schmidt A, Azevedo CF, Cheng A, et al. Infarct tissue heterogeneity by magnetic resonance imaging identifies enhanced cardiac arrhythmia susceptibility in patients with left ventricular dysfunction. *Circulation* 2007;115:2006–14. https://doi.org/10.1161/CIRCULATIONAHA.106.653568; PMID: 17389270.

55. Peters DC, Appelbaum EA, Nezafat R, et al. Left ventricular infarct size, peri-infarct zone, and papillary scar measurements: a comparison of high-resolution 3D and conventional 2D late gadolinium enhancement cardiac MR. *J Magn Reson Imaging* 2009;30:794–800. https://doi.org/10.1002/jmri.21897; PMID: 19787731.

56. Andreu D, Berruezo A, Ortiz-Pérez JT, et al. Integration of 3D electroanatomic maps and magnetic resonance scar characterization into the navigation system to guide ventricular tachycardia ablation. *Circ Arrhythm Electrophysiol* 2011;4:674–83. https://doi.org/10.1161/CIRCEP.111.961946; PMID: 21880674.

57. Fernandez-Armenta J, Berruezo A, Andreu D, et al. Three-dimensional architecture of scar and conducting channels based on high resolution ce-CMR: insights for ventricular tachycardia ablation. *Circ Arrhythm Electrophysiol* 2013;6:528–37. https://doi.org/10.1161/CIRCEP.113.000264; PMID: 23685537.

58. Cochet H, Komatsu Y, Sacher F, et al. Integration of merged delayed-enhanced magnetic resonance imaging and multidetector computed tomography for the guidance of ventricular tachycardia ablation: a pilot study. *J Cardiovasc Electrophysiol* 2013;24:419–26. https://doi.org/10.1111/jce.12052; PMID: 23252727.

59. Yamashita S, Sacher F, Mahida S, et al. Image integration to guide catheter ablation in scar-related ventricular tachycardia. *J Cardiovasc Electrophysiol* 2016;27:699–708. https://doi.org/10.1111/jce.12963; PMID: 26918883.

60. Dall'Armellina E, Karia N, Lindsay AC, et al. Dynamic changes of edema and late gadolinium enhancement after acute myocardial infarction and their relationship to functional recovery and salvage index. *Circ Cardiovasc Imaging* 2011;4:228–36. https://doi.org/10.1161/CIRCIMAGING.111.963421; PMID: 21447711.

61. Lima JA, Judd RM, Bazille A, et al. Regional heterogeneity of human myocardial infarcts demonstrated by contrast-enhanced MRI. Potential mechanisms. *Circulation* 1995;92:1117–25. https://doi.org/10.1161/01.CIR.92.5.1117; PMID: 7648655.

62. Badger TJ, Oakes RS, Daccarett M, et al. Temporal left atrial lesion formation after ablation of atrial fibrillation. *Heart Rhythm* 2009;6:161–8. https://doi.org/10.1016/j.hrthm.2008.10.042; PMID: 19187904.

63. Vunnam R, Maheshwari V, Jeudy J, et al. Ventricular arrhythmia ablation lesions detectability and temporal changes on cardiac magnetic resonance. *Pacing Clin Electrophysiol* 2020;43:314–21. https://doi.org/10.1111/pace.13886; PMID: 32052461.

64. Badger TJ, Daccarett M, Akoum NW, et al. Evaluation of left atrial lesions after initial and repeat atrial fibrillation ablation: lessons learned from delayed-enhancement MRI in repeat ablation procedures. *Circ Arrhythm Electrophysiol* 2010;3:249–59. https://doi.org/10.1161/CIRCEP.109.868356; PMID: 20335558.

65. Kheirkhahan M, Baher A, Goldooz M, et al. Left atrial fibrosis progression detected by LGE-MRI after ablation of atrial fibrillation. *Pacing Clin Electrophysiol* 2019;43:402–11. https://doi.org/10.1111/pace.13866; PMID: 31867751.

66. McGann C, Akoum N, Patel A, et al. Atrial fibrillation ablation outcome is predicted by left atrial remodeling on MRI. *Circ Arrhythm Electrophysiol* 2014;7:23–30. https://doi.org/10.1161/CIRCEP.113.000689; PMID: 24363354.

67. McGann CJ, Kholmovski EG, Oakes RS, et al. New magnetic resonance imaging-based method for defining the extent of left atrial wall injury after the ablation of atrial fibrillation. *J Am Coll Cardiol* 2008;52:1263–71. https://doi.org/10.1016/j.jacc.2008.05.062; PMID: 18926331.

68. Alarcón F, Cabanelas N, Izquierdo M, et al. Cryoballoon vs. radiofrequency lesions as detected by late-enhancement cardiac magnetic resonance after ablation of paroxysmal atrial fibrillation: a case-control study. *Europace* 2020;22:382–7. https://doi.org/10.1093/europace/euz309; PMID: 31821484.

69. Kurose J, Kiuchi K, Fukuzawa K, et al. Lesion characteristics between cryoballoon ablation and radiofrequency ablation with a contact-force sensing catheter: late-gadolinium enhancement magnetic resonance imaging assessment. *J Cardiovasc Electrophysiol* 2020;31:2572–81. https://doi.org/10.1111/jce.14664; PMID: 32648326.

70. Akoum N, Wilber D, Hindricks G, et al. MRI assessment of ablation-induced scarring in atrial fibrillation: analysis from the DECAAF study. *J Cardiovasc Electrophysiol* 2015;26:473–80. https://doi.org/10.1111/jce.12650; PMID: 25727106.

71. Akoum N, Morris A, Perry D, et al. Substrate modification is a better predictor of catheter ablation success in atrial fibrillation than pulmonary vein isolation: an LGE-MRI study. *Clin Med Insights Cardiol* 2015;9:25–31. https://doi.org/10.4137/CMC.S22100; PMID: 25983561.

72. Kamali R, Kump J, Ghafoori E, et al. Area available for atrial fibrillation to propagate is an important determinant of recurrence after ablation. *JACC Clin Electrophysiol* 2021;7:896–908. https://doi.org/10.1016/j.jacep.2020.11.008; PMID: 33640348.

73. Andreu D, Ortiz-Perez JT, Boussy T, et al. Usefulness of contrast-enhanced cardiac magnetic resonance in identifying the ventricular arrhythmia substrate and the approach needed for ablation. *Eur Heart J* 2014;35:1316–26. https://doi.org/10.1093/eurheartj/eht510; PMID: 24394378.

74. Andreu D, Penela D, Acosta J, et al. Cardiac magnetic resonance-aided scar dechanneling: influence on acute and long-term outcomes. *Heart Rhythm* 2017;14:1121–8. https://doi.org/10.1016/j.hrthm.2017.05.018; PMID: 28760258.

75. Berruezo A, Fernandez-Armenta J, Andreu D, et al. Scar dechanneling: new method for scar-related left ventricular tachycardia substrate ablation. *Circ Arrhythm Electrophysiol* 2015;8:326–36. https://doi.org/10.1161/CIRCEP.114.002386; PMID: 25583983.

76. Lardo AC, McVeigh ER, Jumrussirikul P, et al. Visualization and temporal/spatial characterization of cardiac radiofrequency ablation lesions using magnetic resonance imaging. *Circulation* 2000;102:698–705. https://doi.org/10.1161/01.CIR.102.6.698; PMID: 10931812.

77. Celik H, Ramanan V, Barry J, et al. Intrinsic contrast for characterization of acute radiofrequency ablation lesions. *Circ Arrhythm Electrophysiol* 2014;7:718–27. https://doi.org/10.1161/CIRCEP.113.001163; PMID: 24988893.

78. Tao S, Guttman MA, Fink S, et al. Ablation lesion characterization in scarred substrate assessed using cardiac magnetic resonance. *JACC Clin Electrophysiol* 2019;5:91–100. https://doi.org/10.1016/j.jacep.2018.11.001; PMID: 30678791.